https://ntrs.nasa.gov/search.jsp?R=19660008033 2018-07-25T01:48:43+00:00Z

AD

REPORT R-1784

ENERGY ABSORPTION PROPERTIES OF CELLULAR ALUMINUM

by

SAMUEL LIPSON

N66-17322
(ACCESSION NUMBER) (THRU)
41 1
(PAGES) (CODE)
CR 70396 17
(NASA CR OR TMX OR AD NUMBER) (CATEGORY)

November 1965

GPO PRICE $
CFSTI PRICE(S) $
Hard copy (HC) 2.00
Microfiche (MF) .50
ff 653 July 65

NASA Purchase Request L-18,381

(Distribution of this report is unlimited.)

UNITED STATES ARMY
FRANKFORD ARSENAL
PHILADELPHIA, PA.

DISPOSITION INSTRUCTIONS

Destroy this report when no longer needed. Do not return it to the originator.

The findings in this report are not to be construed as an official Department of the Army position unless so designated by other authorized documents.

REPORT R-1784

ENERGY ABSORPTION PROPERTIES OF CELLULAR ALUMINUM

by

SAMUEL LIPSON

NASA Purchase Request L-18381

Distribution of this report is unlimited.

Pitman-Dunn Research Laboratories
FRANKFORD ARSENAL
Philadelphia, Pa. 19137

November 1965

ABSTRACT

17322

The scope of this study covers the optimization of materials and structures of cellular aluminum with respect to applications requiring controlled dissipation of kinetic energy. A design of a linear energy dissipation system is suggested, and its effective operation demonstrated. Conclusions are presented relative to the effect of material properties on energy dissipation characteristics.

Author

TABLE OF CONTENTS

	Page
INTRODUCTION	1
METHODS OF PREPARATION OF MATERIAL	1
Casting Practice	1
Density Control	2
Compression Testing	3
Quality Control	8
Nonaxial Loading	12
RESULTS	16
Tests with Aluminum Separator Plates	16
Tests with Steel Separator Plates	16
DISCUSSION	21
Energy Dissipation	21
Quality Control	23
Cellular Material Density	23
Design of Energy Dissipation Devices	24
CONCLUSIONS	24
APPENDIX A - Recommended Procedures for Preparation of Aluminum Cellular Structures for Energy Dissipation Applications	26
APPENDIX B - Proposed Design for Linear Load Energy Dissipation Device	30
DISTRIBUTION	33

List of Tables

Table		Page
I.	Load-bearing Data for Cellular Structures Prepared with Loosely Packed 40 Mesh Aggregate	13
II.	Load-bearing Data for Cellular Structures Prepared with Compacted 40 Mesh Aggregate	14

List of Illustrations

Figure		
1.	Wax-Aggregate Compaction Method for Density Control of Cellular Metals	4
2.	Effect of Wax-Aggregate Ratio on the Apparent Density of Cellular 7075 Alloy	5
3.	Behavior of Helically Grooved Long Cellular Cylinders under Compression	6
4.	Component Elements and Adhesively Bonded Cellular Metal Cylindrical Stack	7
5.	Compression Test Data Obtained with Adhesively Assembled Cellular Metal Discs	9
6.	Test Record showing Compressive Yield Strength of Cellular Discs	10
7.	Relationship between Disc Weight (Apparent Density) and Load-bearing Characteristics of 7075-T6 Cellular Aluminum	11
8.	Nonaxial Load of 7075-T6 Cellular Aluminum Stacked-disc Assemblies	15
9.	Compression Test of Stacked-disc Assembly, High Density Group, Loosely Packed Aggregate	17
10.	Compression Test of Stacked-disc Assembly, High Density Group, Compacted Aggregate	18
11.	Effect of Load-bearing Characteristics on the Specific Energy Dissipation of Selected Cellular Structures	19
12.	Effect of Load-bearing Characteristics of Cellular Stacked-disc Structures on Specific Energy Dissipation	20
13.	Effect of Apparent Density on Compressive-Yield Strength (2% offset)	20

List of Illustrations (Cont'd)

Figure		Page
14.	Load-deformation Record for Stacked-disc Cylinders with 0.002 inch thick Steel Separators.	22
A-1.	Schematic illustration of Method for Infiltration of Soluble Aggregate and Solidification of Cellular Metal Castings	27
A-2.	Schematic illustration of Leaching Tank Set-up showing Flow of Salt-laden Liquor.	28
B-1.	Energy Dissipation by Deformation of Cellular Aluminum Cylinder	31
B-2.	Load-deformation Record of Linear Energy Dissipation Device	32

INTRODUCTION

This report covers the second phase of a two-year investigation of the energy dissipation characteristics of cellular aluminum alloys. In the first phase,* the compressive properties of cast cellular aluminum alloy cylinders were studied. The principal criterion for material evaluation was high energy absorption at uniform levels of loading through substantially complete destruction of the material. The effects of alloy composition, cell structure, heat treatment, and length/diameter (L/D) ratio were studied. The most promising material was a cast 7075 aluminum alloy, heat treated to high hardness levels.

The purpose of this additional work was to optimize the materials and structures so that: (1) energy dissipation per unit weight of material is increased; (2) the tendency of the material to fail through catastrophic shear is eliminated; and (3) substantially complete deformation of the material (70 percent compression) is accomplished with minimum load build-up. In addition, data were needed on the behavior of these materials under conditions of nonaxial loading, should the design of a specific system require such loading.

A further objective of this phase was to broaden the range of apparent density that could be achieved with the process in order to provide greater freedom of design in practical applications for the materials. The material prepared during the earlier study had an apparent density between 0.85 and 0.95 g/cc with a uniform cell structure. It was considered desirable to retain the uniform cell structure and, at the same time, lower the apparent density of the material. Several possible methods for achieving lower density were suggested during the earlier investigation. However, none of these was found to be entirely satisfactory. The present approach to this problem is somewhat different than those tried earlier. The method is detailed in this report.

METHODS OF PREPARATION OF MATERIAL

Casting Practice

One of the characteristics of the method employed for preparation of the cellular material is that the solidification rate of the alloy is necessarily slow. Infiltration is accomplished with the aggregate temperature slightly above the melting point of the alloy. It was thought that there might be some improvement in material properties if

*S. Lipson, "Cellular Aluminum for Use in Energy Dissipation Systems," Frankford Arsenal Report R-1716 (NASA Contractor Report CR-93, Sep 64), April 1964.

the solidification rate could be accelerated. This appeared to be especially important because the most promising aluminum alloys for the energy dissipation applications were those of the 7000 series. These are highly alloyed materials (Al-Zn-Mg-Cu) which normally require extensive working and heat treatment in order to realize the optimum combination of mechanical properties.

The slow solidification rate inherent in the cellular metal process tends to result in a coarse structure. The coarse structure is difficult to solutionize effectively, especially since no mechanical working can be employed between casting and heat treatment. It was hoped that if solidification rates were increased, the resulting refinement of the structure would improve the effectiveness of the heat treatment. Efforts to refine the structure, however, were not successful. It was therefore decided that the material processed for use in this investigation would be handled in the same manner as for the earlier study.

Density Control

The earlier study reviewed, in some detail, a number of potential methods for decreasing the apparent density of the cellular metal. The only effective method found for reducing the apparent density of the material, however, was one which introduced salt particles small enough to fit into the interstices of the larger salt particles in the aggregate. This resulted in a metal structure of nonuniform cell size. Subsequent tests of these structures revealed that these structures were undesirable because of their deformation characteristics and the fact that it was important to retain the uniform cell size distribution in the cellular structure.

Briefly reviewing the factors which affect the density of the cellular structures, the tap density achieved in filling the mold with the granular aggregate is the primary factor affecting the apparent density of the cellular metal which is cast into the aggregate. The higher the tap density of the aggregate, the lower will be the apparent density of the metal structure.

It was found that the salt particles, which make up the aggregate, pack in very nearly the same manner that would be predicted from a model based upon assuming spherical particles of uniform size. Under these conditions, the particles account for approximately two-thirds of the volume of the cavity they occupy. If it were possible to effect further compaction of the aggregate over that resulting from the simple nesting of the particles, more of the aggregate could be packed into the mold cavity, less volume would be available for the infiltrating molten metal and, hence, a lower density cellular metal structure would result.

A method for controlling the compaction of the granular salt aggregate was therefore sought. One such method was found which proved to be practical and controllable. Using this method, a homogeneous mixture of salt aggregate and a measured quantity of melted wax was prepared. This mixture was precast into a cylindrical mold and allowed to solidify. The cast cylinder was then compacted under a pressure of 40,000 psi. Under these conditions, the wax-salt mixture became fully compacted, as shown in Figure 1.

The compact was then fired at a temperature of 1250° F to oxidize the wax component of the mixture. The remaining salt was in the form of a sintered briquette, and is also shown in Figure 1. Examination of this briquette shows that the particles are practically unaltered in shape, except that they are arranged in a more compact form and the outer particles conform to the curvature of the cylinder wall. There is no evidence of fracturing of the salt crystals. The volume of void space existing between the particles was found to be equivalent to the volume of wax introduced into the original mixture. This compacted briquette may be compared with the appearance of the loosely packed and sintered briquette, also shown in Figure 1.

The extent of density control possible with the wax method is shown in Figure 2. The points represent cellular aluminum prepared from 30 mesh salt plus various amounts of wax. The slope of the line drawn through the data points is such that an extrapolation of the line would cause it to intersect the origin. This is further evidence that the apparent density of the cellular structure is ~~inversely~~ proportional to the quantity of wax introduced into the mixture.

Compression Testing

In general, cellular aluminum alloy structures can be uniformly compressed as much as 70 percent of the specimen length. In the case of ductile compositions, this type behavior is characteristic for columns having a length-to-diameter ratio (L/D) up to approximately 2.5. With columns having a greater slenderness ratio, a buckling tendency develops comparatively early in the test. With stronger alloys, which are inherently less ductile, a tendency for shear failure develops early in the loading cycle. This was observed even when the L/D ratio was as small as 1.0. Premature failures such as these limit the deformation that can be realized in the material and, consequently, the potential for dissipation of energy is similarly limited. In the case of the higher strength materials, the severe limitations governing their slenderness ratio would also limit the stroke that could be tolerated in an energy dissipation device.

Neg: 36.231.S1274/ORD.65

Pressure-compacted Aggregate

Loosely Packed Aggregate

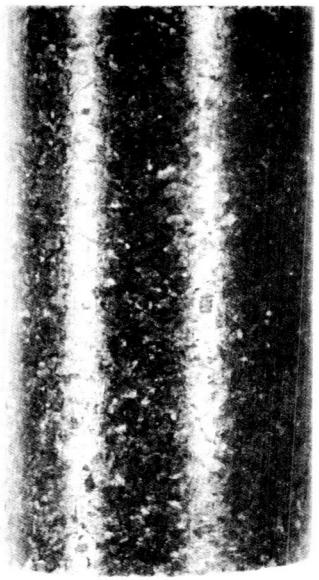

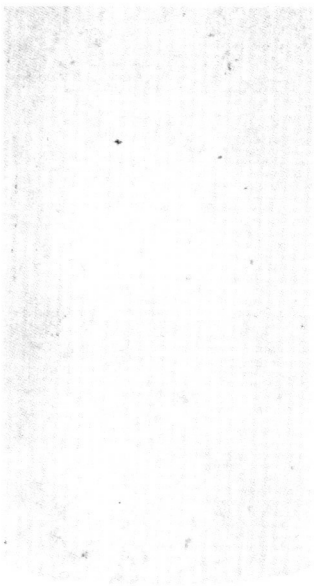

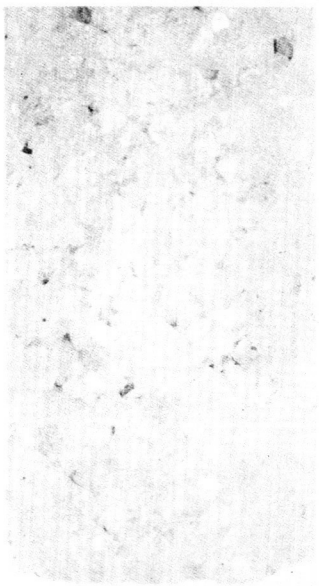

As-pressed (with Wax)

Sintered

Sintered

12 mesh Aggregate

Mag: 1X

Figure 1. Wax-Aggregate Compaction Method for Density Control of Cellular Metals

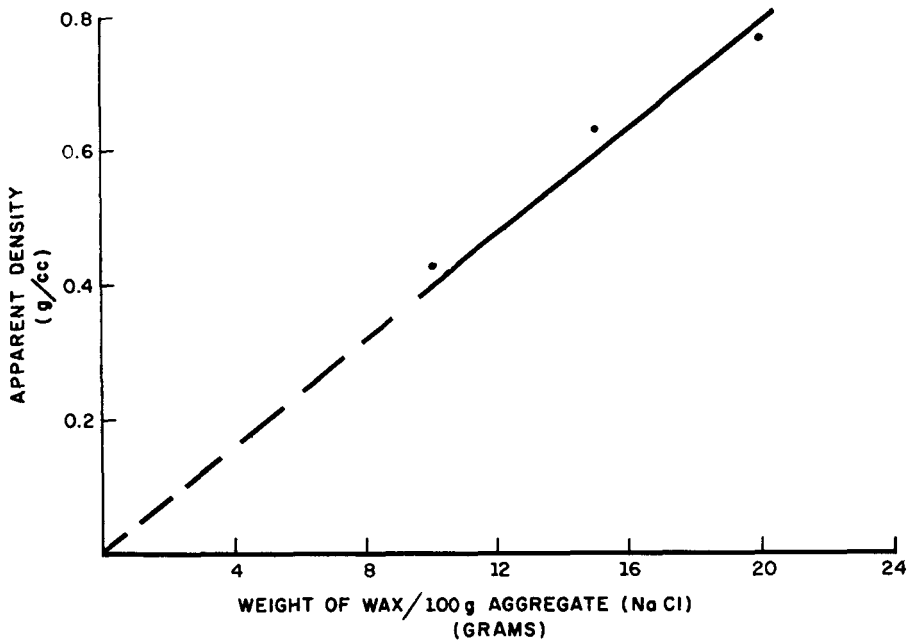

Figure 2. Effect of Wax-Aggregate Ratio on the Apparent Density of Cellular 7075 Alloy

One of the methods examined for coping with these problems was to machine circumferential grooves into the cylinder. It was thought that uniform compression of the test cylinder would be favored by these grooves and, thereby, would inhibit the formation of shear planes. Cylinders, machined with both helical and circumferential grooves, were tested. It was found that these grooves were of no benefit for inhibiting the shear planes in high strength materials and actually promoted columnar instability in the lower strength ductile alloys. Figure 3 shows two such test pieces. The ductile alloy (356, as cast) shows the columnar instability, and the high strength alloy (7075-T6) shows the characteristic shear failure always encountered with longer columns.

As a result of this and other studies of the problem, a reasonable solution was evolved by preparing columns which were made up of a series of disc elements, each having an L/D ratio of 0.2 to 0.5. The discs in the columns were separated from each other by solid 0.025 inch thick 2024-T4 sheet material. These elements were assembled into stacks by adhesively bonding the assembly. Figure 4 shows the component elements of this system and an adhesively assembled stack.

In order to evaluate this system, a number of assembled stacks of discs were tested. The separator plates were prepared with either a single 3/16 inch hole at the center or with a series of four holes

Neg: 36.231.S1275/ORD.65

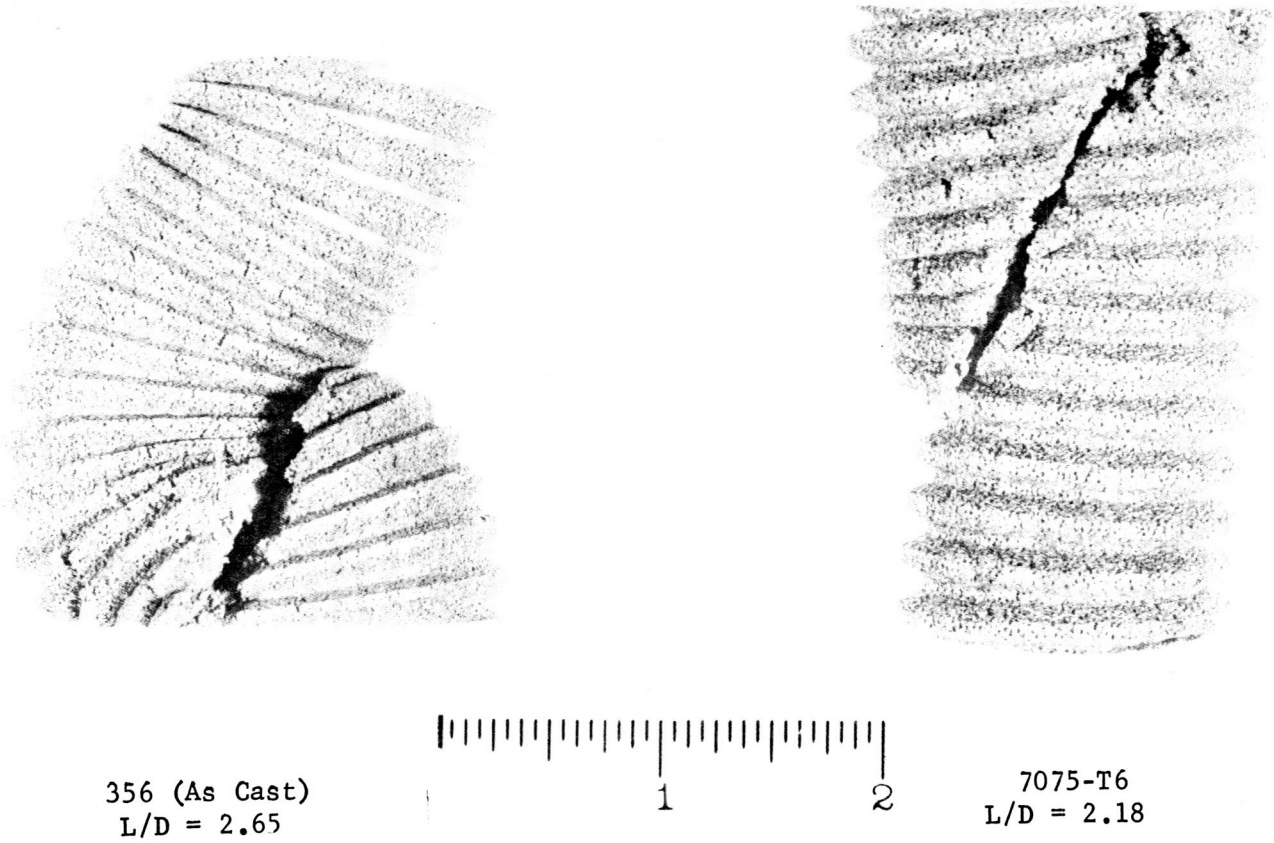

Figure 3. Behavior of Helically Grooved Long Cellular Cylinders under Compression

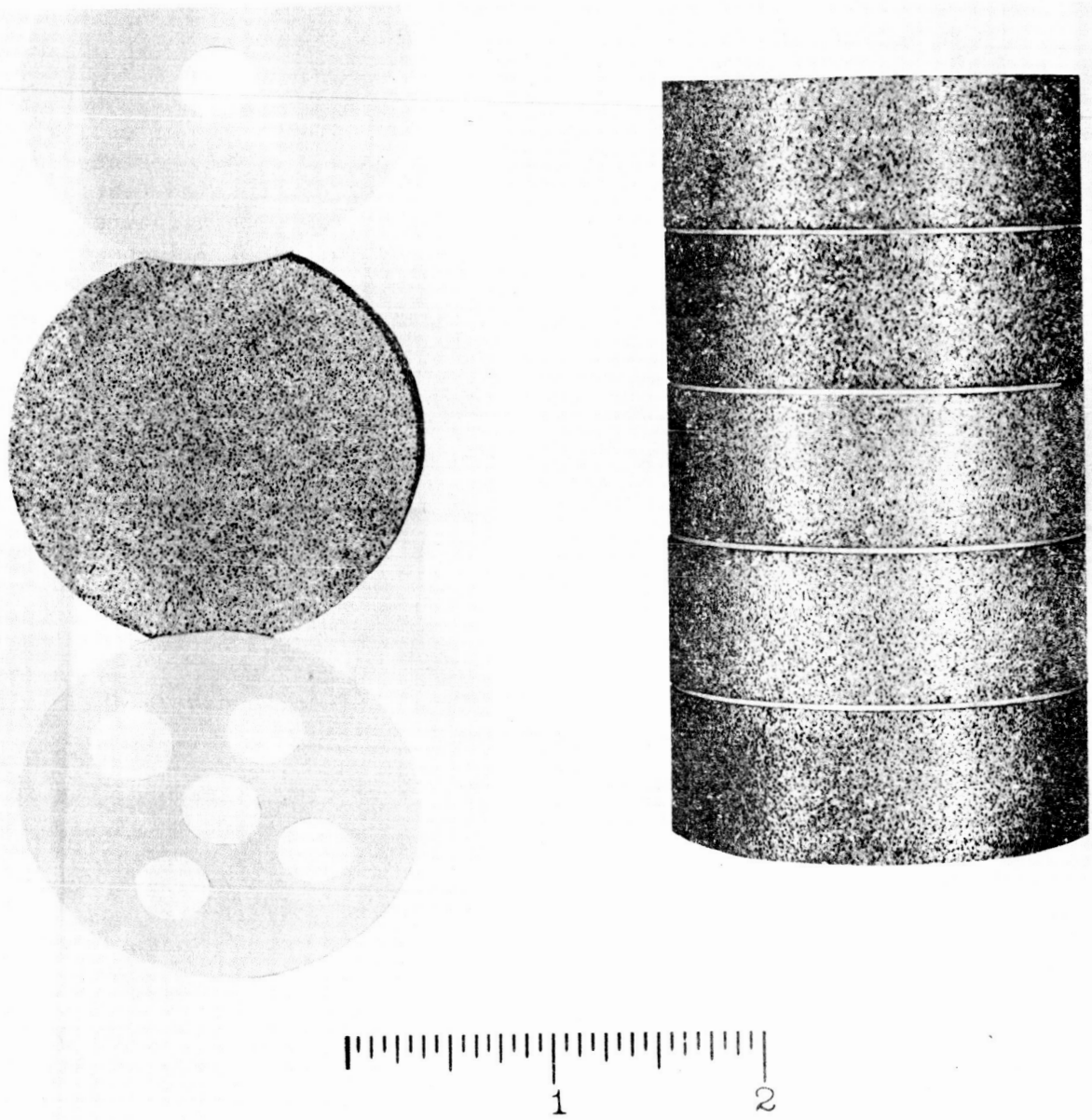

Figure 4. Component Elements and Adhesively Bonded Cellular Metal Cylindrical Stack

radially located around the center hole. Figure 4 shows both the one-hole and the five-hole plates. The L/D ratio of these composite cylinders was approximately 2. Two-inch diameter cellular discs were employed, using disc thicknesses of 1/2 and 3/4 inch. Figure 5 shows the load deformation curves obtained in testing these composite cylinders. The compression samples are also shown in this figure.

Although there is some evidence of a tendency toward columnar instability, the formation of catastrophic shear planes was effectively inhibited. Later in this report additional data will be presented on the behavior of the stacked-disc assembly under compression testing. It was tentatively decided from this series of tests that future stacked-disc assemblies would employ component discs of 2 inches diameter by 3/4 inches long, and that the one-hole separator plate would be used. Tests indicated that the five-hole plates were not necessary to key the assembly during compressive loading.

Quality Control

Compression tests conducted with the stacked-disc assemblies often showed that one or more of the discs in the stack would be almost completely collapsed before there was much evidence of deformation in the companion discs. There were a number of possible explanations for the variability in behavior, the principal possible sources for this variability being casting quality, heat treatment effectiveness, and material density.

Every reasonable effort was made to standardize procedure, but it was obvious that sufficient differences in quality of the material existed to lead to differences in material behavior under compression. In order to avoid the delays that might be expected in trying to track down and control all possible causes for this variability, it was decided to devise a test for predicting the behavior of the material.

This was accomplished by determining the load that each disc could support at some small increment of deformation. This was done by pretesting the disc and recording the load at 2.0 percent permanent set. Figure 6 shows a typical data chart recorded with a series of such tests. The selection of discs was random from a given lot, and the disc diameters were easily controlled to 2.062 ± 0.003 inches. The slices were sawed to a nominal 3/4 inch thickness, plus or minus 1/64 inch. In order to determine if any correlation existed between the load measurement and the disc weight, the data were plotted as shown in Figure 7. This shows a well defined band of values, correlating load with disc weight and density.

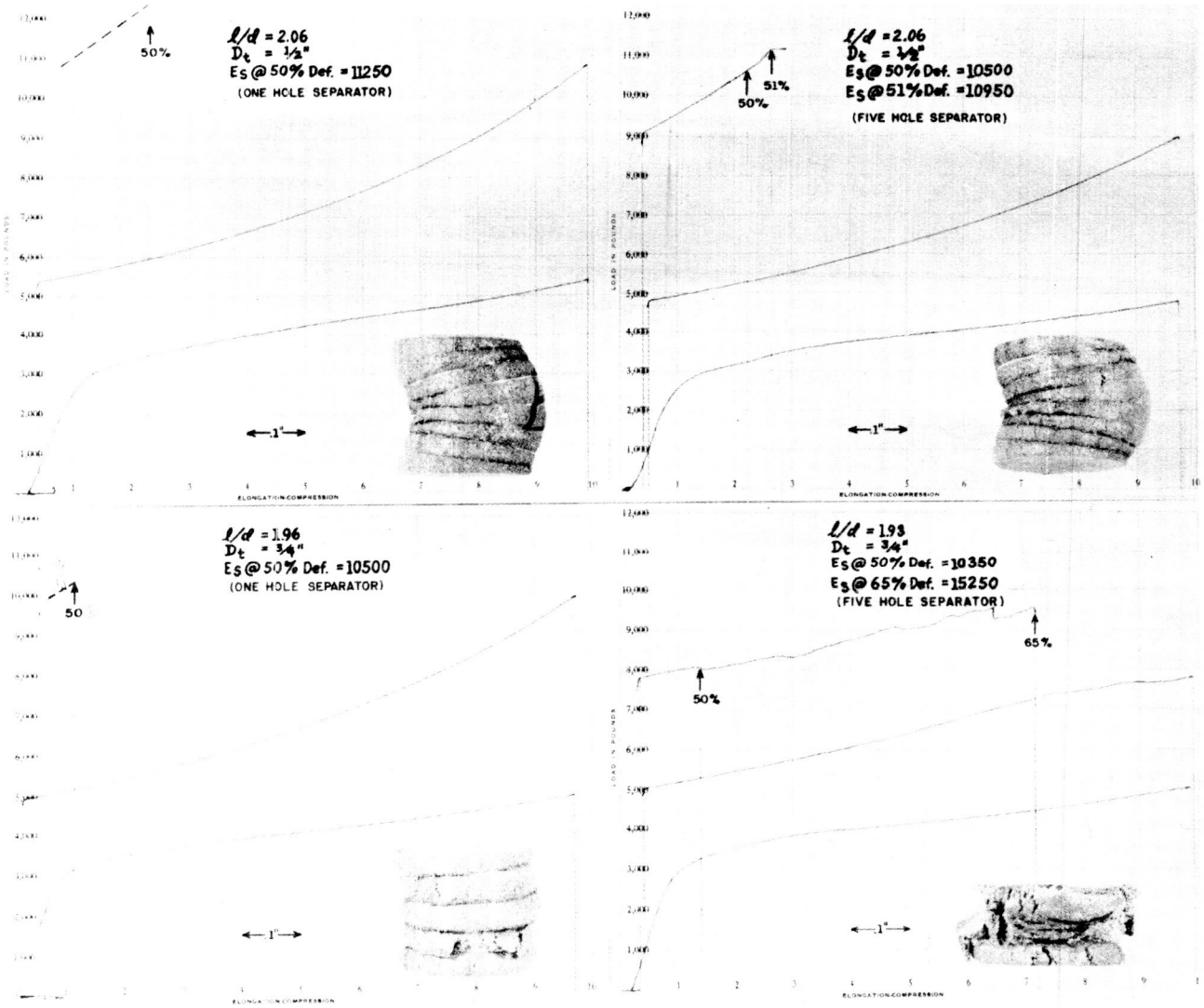

Cell size: 30 Mesh Alloy: 7075-T6

E_s = Specific Energy (ft-lb/lb) D_t = Disc Thickness

Actual Load - Load in pounds X 5

Figure 5. Compression Test Data Obtained with Adhesively Assembled Cellular Metal Discs

(Crushed specimen illustrated shows appearance of stack at end of the test.)

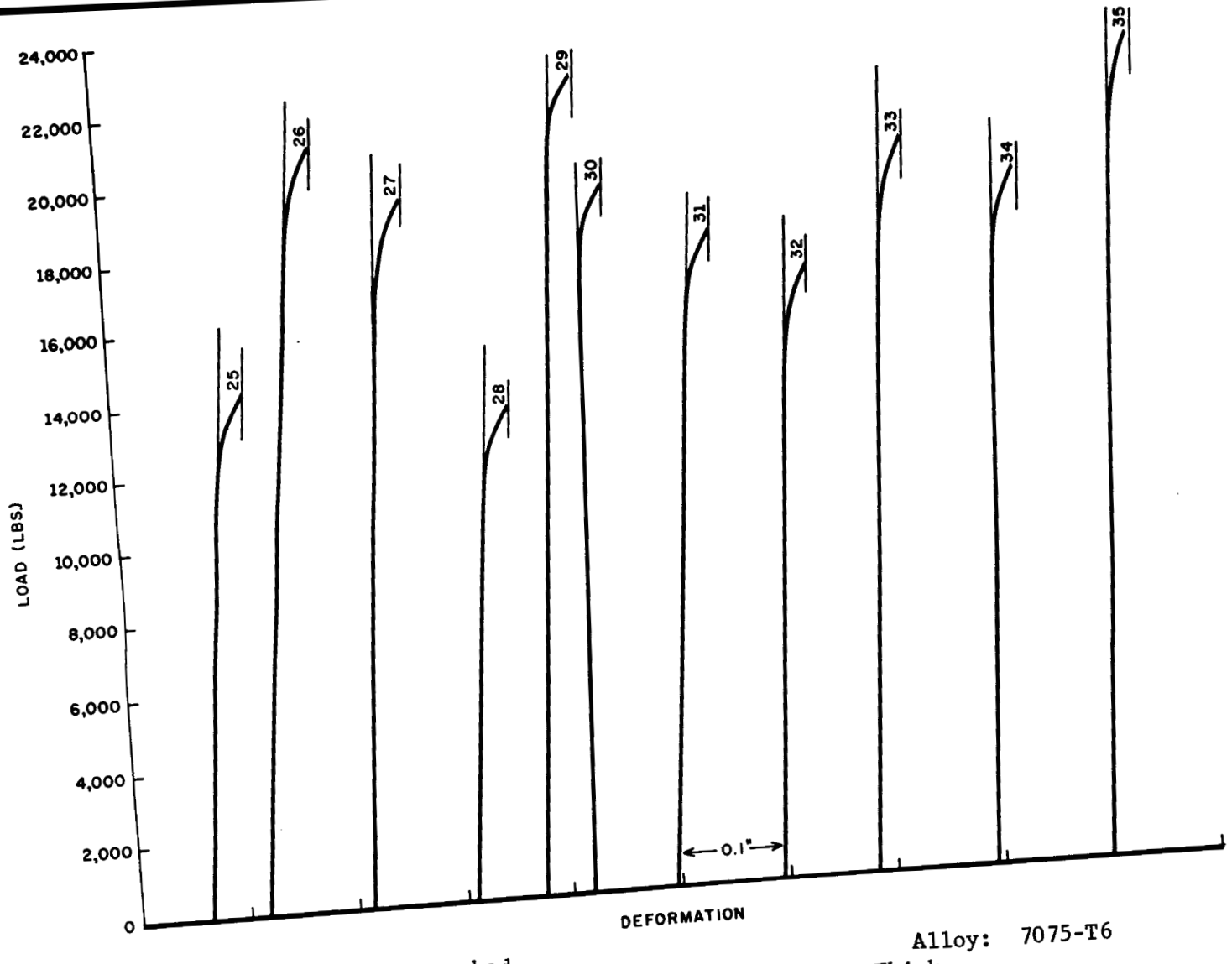

Alloy: 7075-T6

Aggregate: Loosely packed
Disc Size: 2.062 in. Dia X 0.75 in. Thick

Figure 6. Test Record showing Compressive Yield Strength of Cellular Discs

N.B. Test continued to 2% deformation. Specimen numbers refer to Table I.

Neg: 36.231.51714/ORD.65

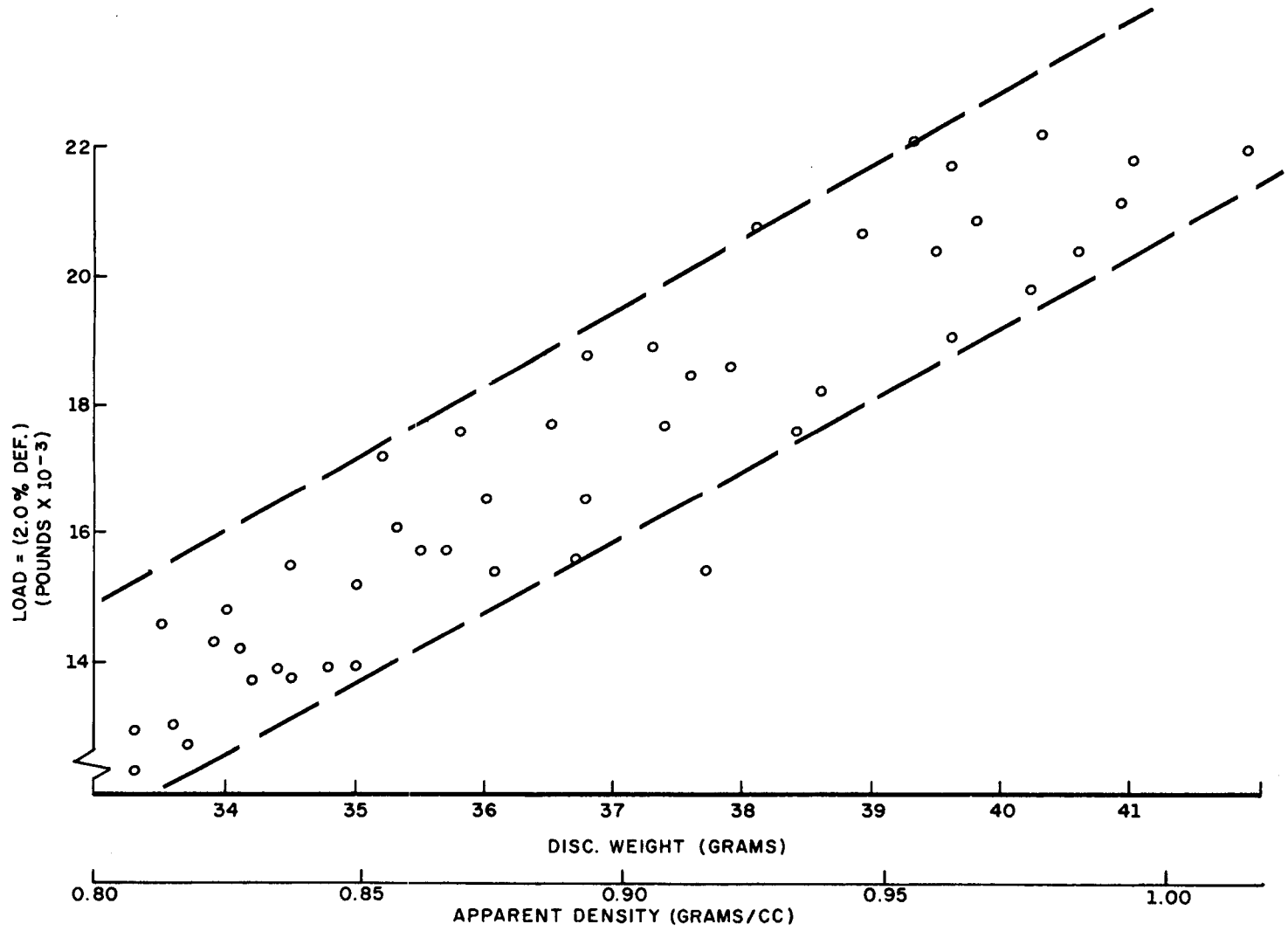

Cell size: 40 mesh; Disc size: 2.062 in. dia x 0.75 in. thick; Nominal density: 0.95 g/cc, loosely packed

Figure 7. Relationship between Disc Weight (Apparent Density) and Load-bearing Characteristics of 7075-T6 Cellular Aluminum

Neg: 36.231.S1528/ORD.65

It is therefore apparent that the principal reason for the variability in compressive behavior is associated with the density variation observed in the study of the individual discs. By selective grouping of the cellular discs on the basis of density (i.e., compressive yield strength), it is possible to prepare columns where each of the component discs would deform uniformly under compressive loading. A more precise examination of the relationship between material density and compressive yield strength will be presented later in this report.

Table I gives the loads, weights, and disc numbers for a lot of 50 discs employed for one series of tests. These represented a structure prepared with an uncompacted 40 mesh aggregate having a nominal density of 0.95 g/cc. Table II presents similar data on a group of discs prepared with a compacted aggregate of the same cell size having a nominal density of 0.75 g/cc. Both of these Tables are presented in descending order of load rating. The performance of these discs in assembled stacks will be discussed later in this report.

Nonaxial Loading

The design of an energy dissipation system using a stacked disc column must take into account the possibility that it may be loaded at some angular displacement from axiality. For this reason a qualitative evaluation was attempted in order to assess the consequences of such loading. These specimens were loaded between the compression platens of a 60,000-pound tensile testing machine. The axial load displacement was effected by fixing to the platens wedges which formed a 10° angle with the surface of the platens. The surfaces of these wedges were serrated to prevent slippage of the specimen. However, it was found that the large horizontal force component caused the testing machine screws to bind and it was necessary to scale down the standard two-inch diameter specimens used for the other phases of this study.

A series of 1.5 inch diameter stacked disc assemblies with L/D ratios ranging between 1 and 2 were prepared. It was found that the specimens with the lower L/D ratios accommodated to the nonaxial loading and deformed in a manner similar to those which were loaded axially. The longer specimens, however, developed a shear plane early in the test, causing the load to fall off precipitously. Figure 8 is a photograph of typical specimens, showing the observed behavior. The specimen with an L/D of 1.97 was removed from the testing machine platens just before it would have separated into two segments.

TABLE I. Load-bearing Data for Cellular Structures Prepared with Loosely Packed 40 Mesh Aggregate (7075-T6 Alloy; 0.95 g/cc Nominal Density)

Spec No.	Load* (lb x 10^{-3})	Weight (g)	Spec No.	Load* (lb x 10^{-3})	Weight (g)	Spec No.	Load* (lb x 10^{-3})	Weight (g)
16	22.2	40.3	1	18.5	37.6	38	15.4	36.1
29	22.1	39.3	50	18.2	38.6	7	15.2	35.0
35	22.1	42.6	43	17.7	37.4	45	14.8	34.0
23	22.0	41.9	44	17.7	36.5	40	14.6	33.5
20	21.8	41.0	17	17.6	38.4	6	14.3	33.9
47	21.7	39.6	31	17.6	35.8	37	14.2	34.1
10	21.1	40.9	13	17.2	35.1	2	13.9	34.4
5	20.9	39.8	22	16.5	36.0	9	13.9	32.9
26	20.8	38.1	32	16.5	36.8	24	13.9	35.0
3	20.7	38.9	14	16.1	35.2	25	13.9	34.7
11	20.4	40.6	4	15.7	35.5	46	13.9	33.3
49	20.4	39.5	39	15.7	34.7	19	13.7	34.2
33	19.8	40.2	42	15.7	35.7	36	13.7	34.5
30	19.0	39.6	21	15.6	36.7	28	13.0	33.6
27	18.9	37.3	41	15.6	34.5	48	12.7	33.7
18	18.8	36.8	15	15.5	34.5	8	12.3	33.3
34	18.7	37.9	12	15.4	37.7			

*Compressive yield load on 2.06 inch diameter cylinder (2.0% offset).

TABLE II. Load-bearing Data for Cellular Structures Prepared with Compacted 40 Mesh Aggregate (7075-T6 Alloy; 0.75 g/cc Nominal Density)

Spec No.	Load* (lb x 10^{-3})	Weight (g)	Spec No.	Load* (lb x 10^{-3})	Weight (g)	Spec No.	Load* (lb x 10^{-3})	Weight (g)
29	13.1	32.8	7	9.2	30.0	13	7.5	27.5
44	12.7	30.2	39	9.2	27.2	19	7.5	26.2
6	12.6	32.0	21	9.1	26.8	43	7.4	24.5
1	12.0	31.1	35	9.0	27.3	48	7.4	26.3
27	11.6	30.3	22	8.8	27.4	50	7.3	27.2
23	11.1	32.6	24	8.7	28.3	25	7.2	25.1
8	11.0	29.8	5	8.5	25.6	46	7.2	25.4
9	10.9	30.0	36	8.4	26.2	32	6.5	26.8
49	10.2	27.0	42	8.4	25.5	45	6.5	25.9
27	10.1	28.3	20	8.3	26.1	33	6.1	24.5
2	10.1	29.8	30	8.3	26.9	34	6.0	23.9
16	9.9	28.0	3	8.1	26.1	18	5.9	26.2
4	9.7	28.5	47	8.1	27.5	17	5.8	25.5
41	9.7	28.1	40	8.0	25.4	14	5.7	26.1
11	9.4	27.5	15	7.9	26.8	38	5.1	24.0
12	9.4	28.0	31	7.9	26.5	28	4.9	24.2
26	9.4	27.3	10	7.6	25.3			

*Compressive yield load on 2.06 inch diameter cylinder (2.0% offset).

Neg: 36.231.S1277/ORD.65

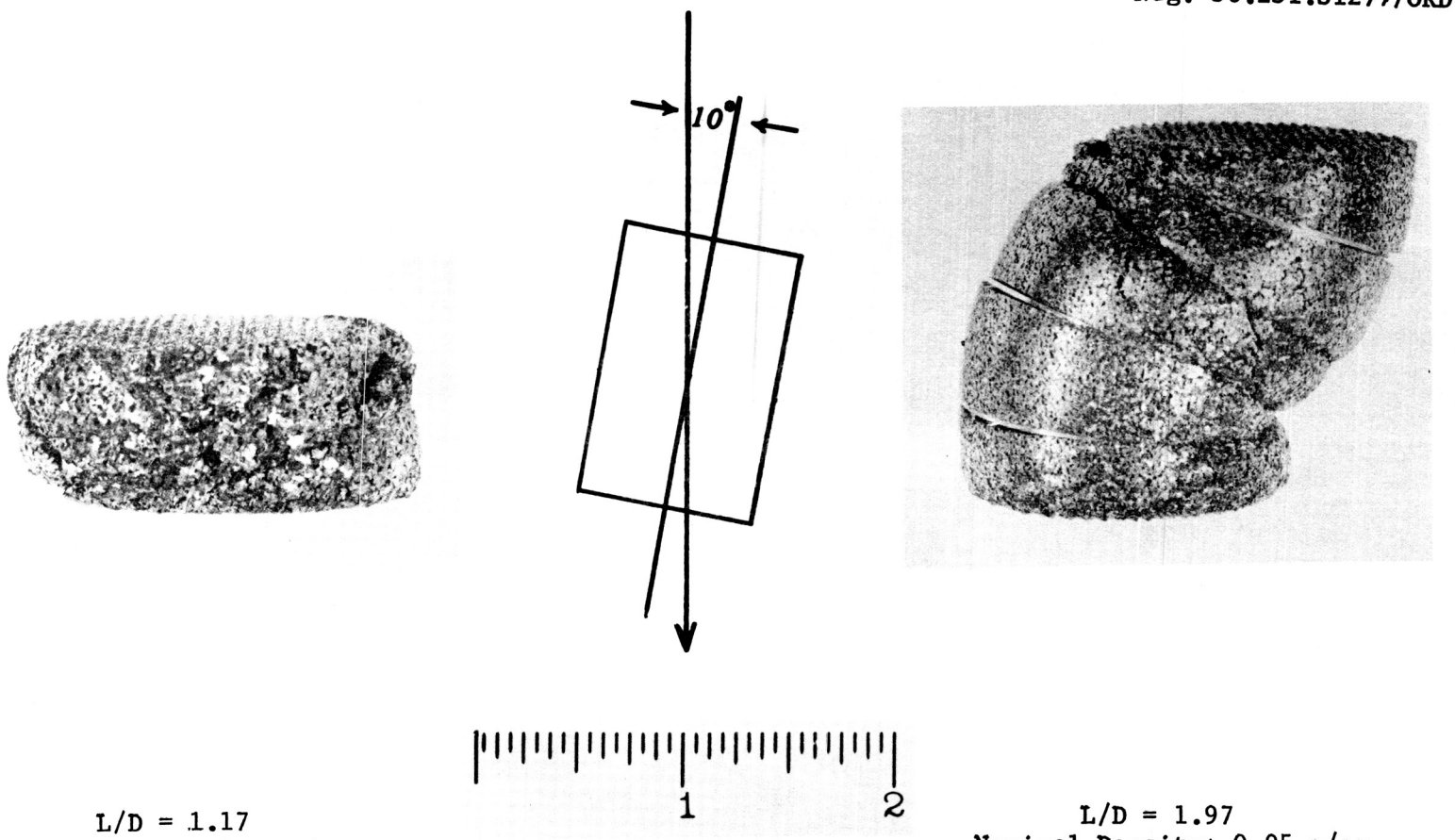

L/D = 1.17
Cell size: 30 Mesh

L/D = 1.97
Nominal Density: 0.95 g/cc

Figure 8. Nonaxial Load of 7075-T6 Cellular Aluminum Stacked-disc Assemblies

RESULTS

Tests with Aluminum Separator Plates

The energy dissipation potential of the cellular structures was determined for the two groups of discs listed in Tables I and II. In order to evaluate the effect of disc density, selected groups of five discs each were assembled into test cylinders. The groupings represent the highest load-bearing material and the lowest load-bearing material in each of the two lots of material. In addition, groups representing the middle values were assembled and similarly tested.

Figure 9 shows the load deformation record obtained for the higher strength group taken from the 0.95 g/cc density material. Photographs of the test cylinder were taken at a series of compression increments and are shown with the test record. Figure 10 shows a similar test record obtained with the group of discs representing the lower density lot (0.75 g/cc). These samples also represent the high group from this lot.

The specific energy dissipation (ft-lb/lb) of these tests groups was calculated and the data have been plotted in Figure 11. Each point on the curve represents the cumulative energy dissipation resulting from the cylinder deformation at that point. The curves show that the load-bearing rating, as determined by the compressive-yield strength, correlates well with the energy dissipation characteristics of the stacked disc cylinders.

In order to show more clearly the effect of the compressive-yield strength of the component discs on the energy dissipation characteristics, the specific energy values at 50 and 70 percent deformation are plotted in Figure 12 as a function of the average yield strength of the discs which make up the stack. The points are representative of two nominal density groups and three density levels selected from each group. These data show that specific energy dissipation correlates directly with compressive-yield strength. The measured compressive-yield strength of the component discs can also be correlated directly with the apparent density of the material. Figure 13 shows a plot of compressive-yield strength as affected by the apparent density of the cellular material.

Tests with Steel Separator Plates

In order to evaluate the effect of the separator material on the energy dissipation characteristics, two stacks of cylinder were assembled using 0.002 inch thick steel foil separators. The component discs

Neg: 36.231.S1713/ORD.65

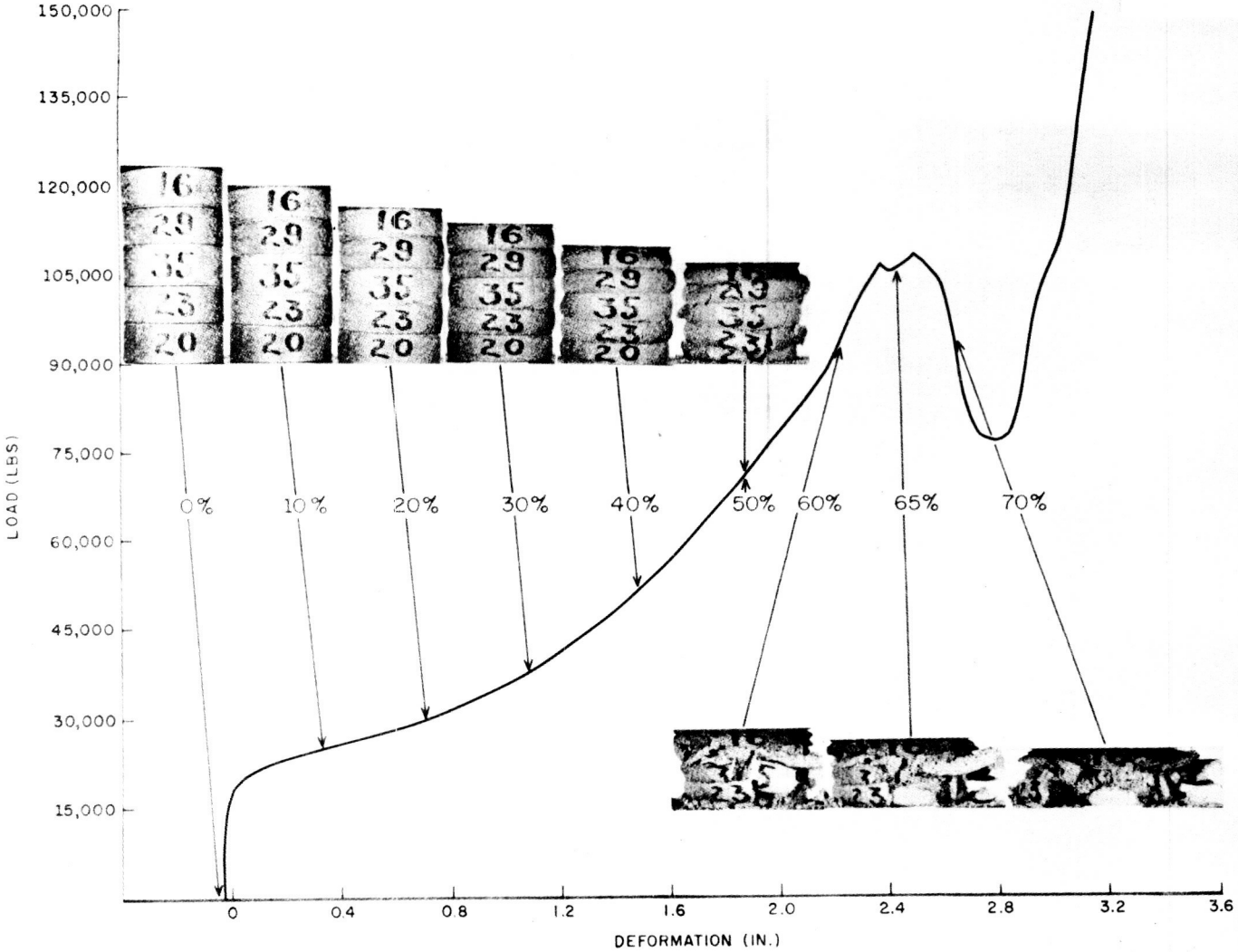

Alloy: 7075-T6 L/D: 1.84 Weight: 221.1 g
Disc diameter: 2.06 inch Stack height: 3.80 inches

Figure 9. Compression Test of Stacked-disc Assembly, High Density Group, Loosely Packed Aggregate

Neg: 36.231.S1715/ORD.65

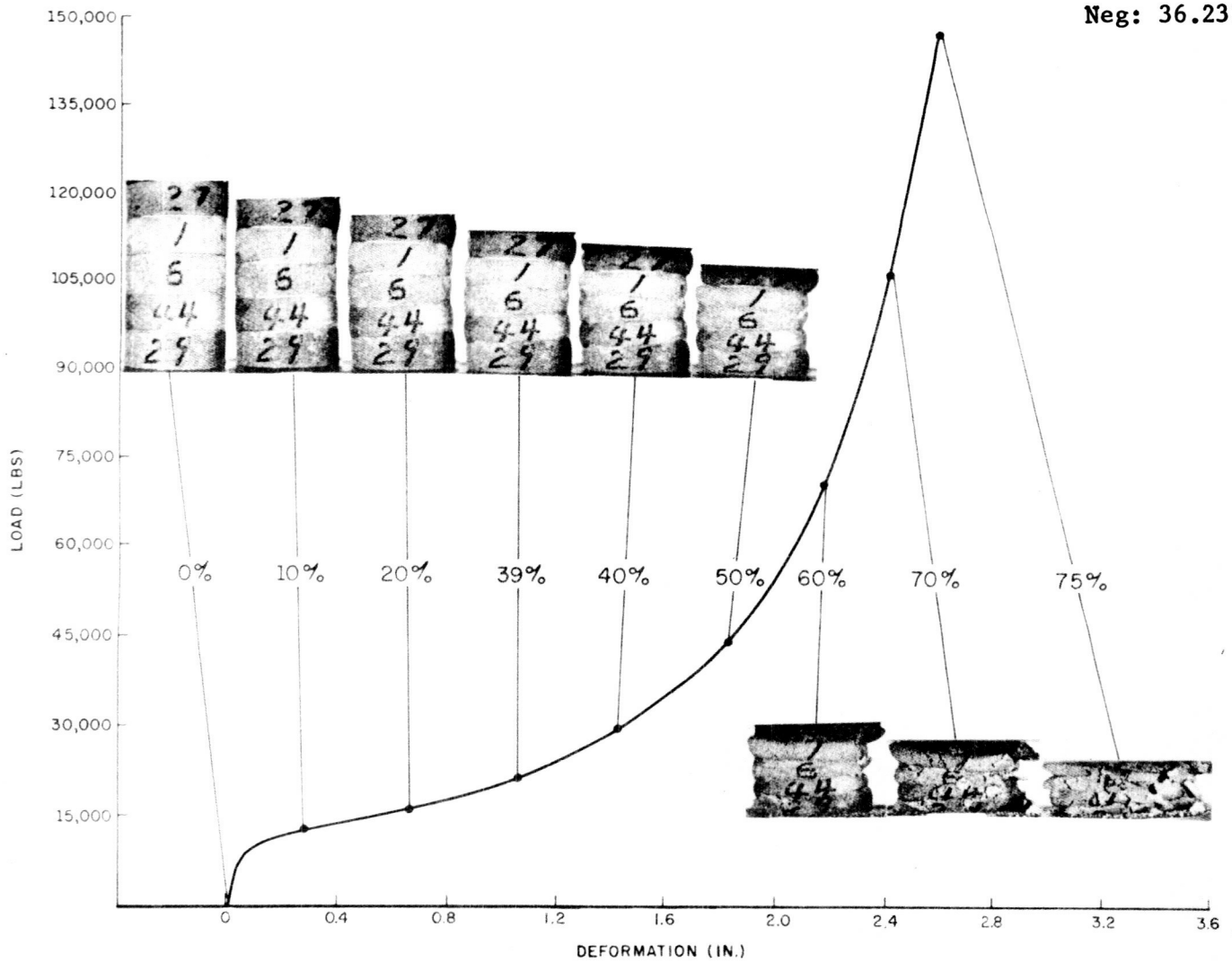

Alloy: 7075-T6 L/D: 1.78 Weight: 172.9 g
Disc diameter: 2.06 inch Stack height: 3.67 inches

Figure 10. Compression Test of Stacked-disc Assembly, High Density Group, Compacted Aggregate

Neg: 36.231.S1529/ORD.65

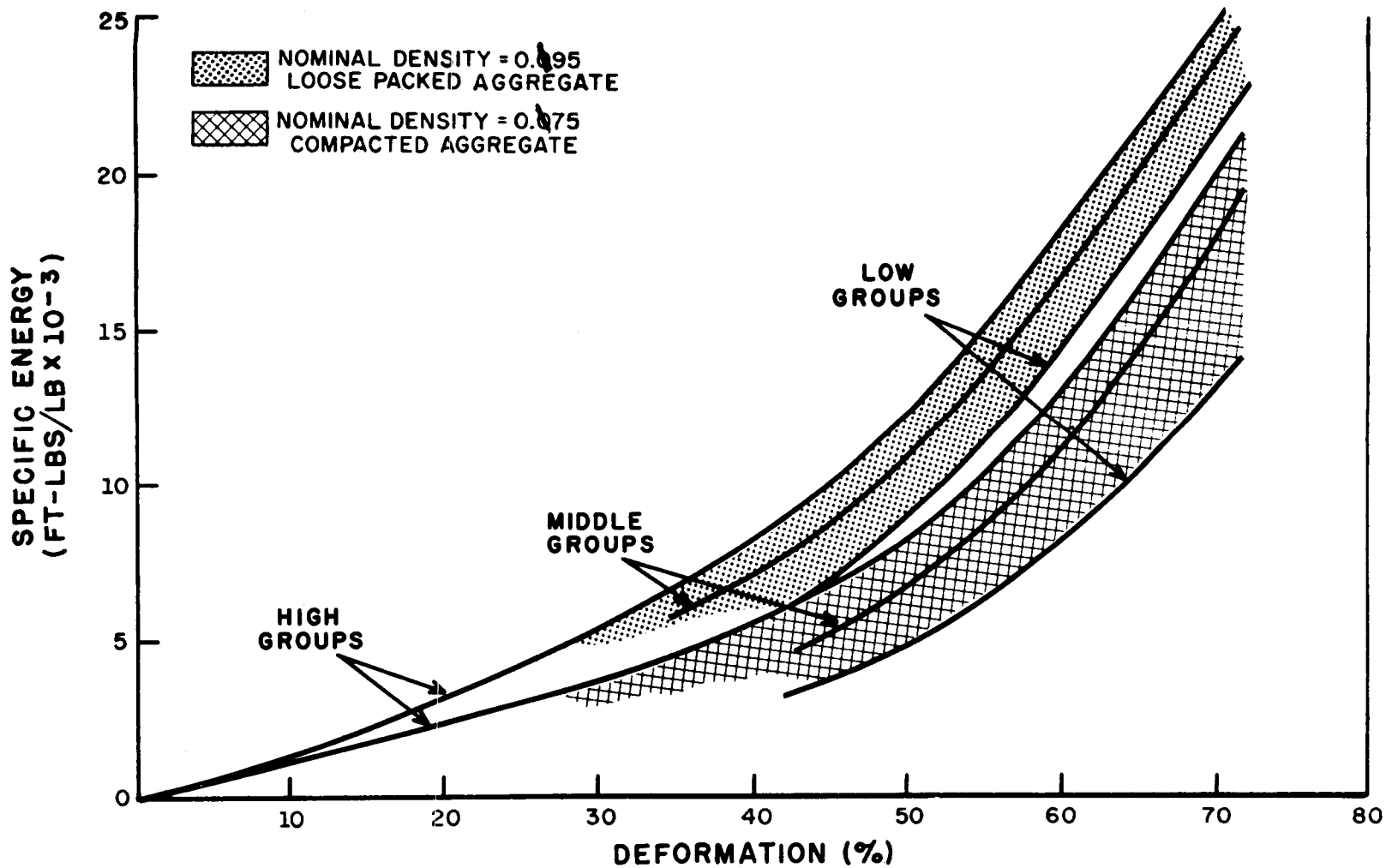

Cell size: 40 Mesh

Alloy: 7075-T6

Figure 11. Effect of Load-bearing Characteristics on the Specific Energy Dissipation of Selected Cellular Structures

Neg: 36.231.S1530/ORD.65

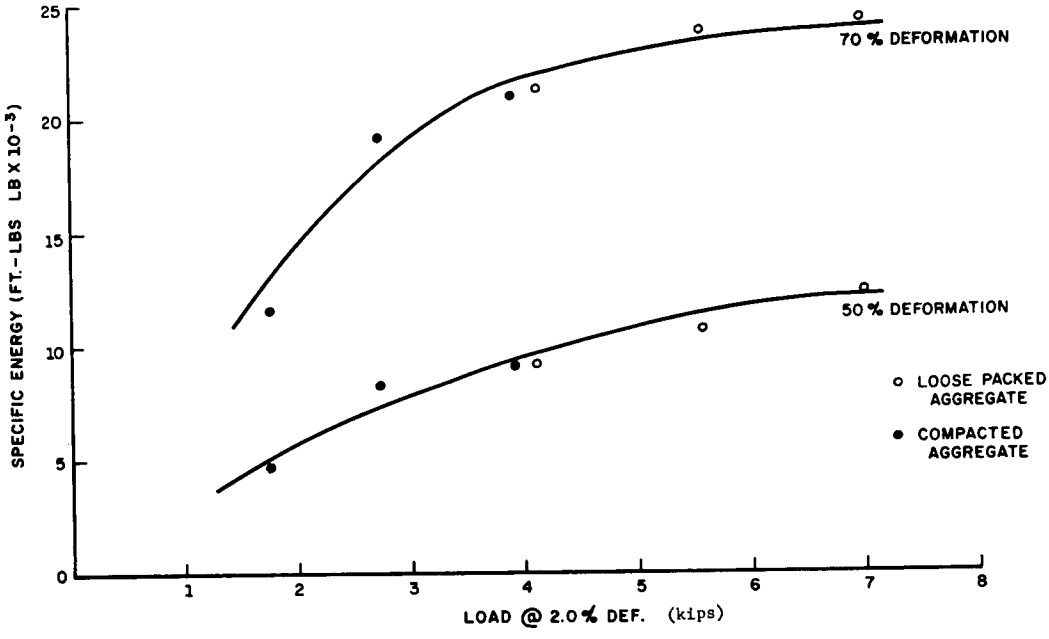

, Cell size: 40 Mesh

Alloy: 7075-T6

Figure 12. Effect of Load-bearing Characteristics of Cellular Stacked-disc Structures on Specific Energy Dissipation

Neg: 36.231.S1531/ORD.65

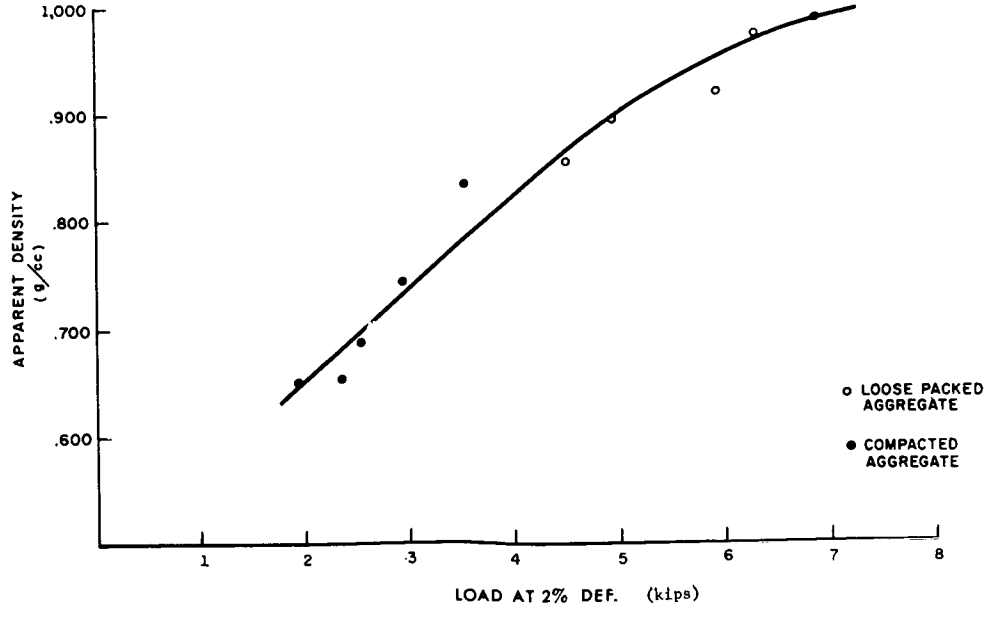

Alloy: 7075-T6

Figure 13. Effect of Apparent Density on Compressive-Yield Strength (2% offset)

were representative of the middle yield strength group from each of the two lots of discs listed in Tables I and II.

Figure 14 shows the load deformation chart record obtained with these tests. The thin steel separator does not provide the support obtained with the heavier aluminum separators. As a result, there is a tendency for the component discs to break up, rather than deform as was the case with the aluminum separators.

These steel disc separators, however, do serve to inhibit the catastrophic shear failure observed with the continuous cellular columns. The test record shows that the load build-up is also inhibited for deformations up to 70 percent. The break-up of the structure, of course, results in less efficient utilization of the material. As a consequence, the energy dissipation resulting from these compression tests is substantially lower than when aluminum separators were used. The specific energy dissipation at 50 and 70 percent deformation for both the thin steel separator and the aluminum disc separator columns follows.

Deformation (%)	Specific Energy (ft-lb/lb)			
	0.75 g/cc Structure		0.95 g/cc Structure	
	Steel	Aluminum	Steel	Aluminum
50	5,200	7,000	6,900	11,500
70	7,300	18,500	9,000	23,500

DISCUSSION

Energy Dissipation

One of the objectives of this study of the deformation characteristics of cellular metals was to develop a structure that would tend to absorb energy at a relatively constant load level. A parallel objective was that the specific energy dissipation be high in relation to that of other materials being considered for this purpose.

On the basis of these tests, it must be concluded that these objectives are fundametnally contradictory for the cellular material. If deformation of the structure proceeds with maximum involvement of the material in the structure (as with the aluminum separators), the resulting compaction raises the load-bearing capacity of the structure. Hence, the load tends to rise as deformation proceeds. Under conditions where the material involvement is less efficient and a considerable amount of fragmentation occurs (as with the thin steel separators), the tendency for the load to increase diminishes.

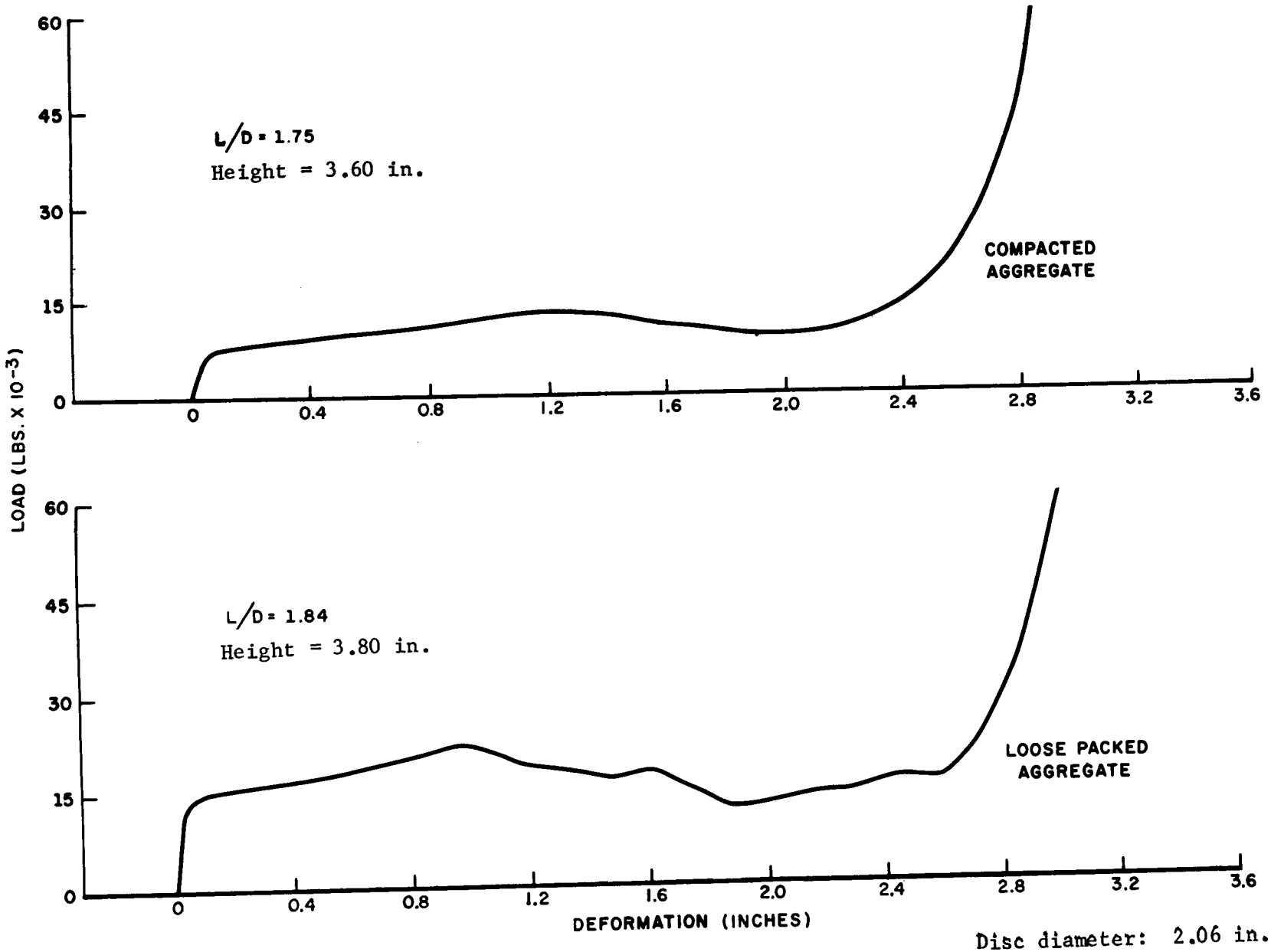

Disc diameter: 2.06 in.

Figure 14. Load-deformation Record for Stacked-disc Cylinders with 0.002 inch thick Steel Separators

Neg: 36.231.S1667/ORD.65

Quality Control

A correlation exists between yield strength of the cellular structure and the energy dissipation resulting from compression of the structure. Since there is also a correlation between yield strength and density, it makes possible the employment of the density parameter as a measure of the energy dissipation potential of the material. The correlation of density with yield strength of the material suggests a method for quality assurance control of materials of this type.

Under production conditions, it should be desirable to control the disc dimensions to very close limits. This simplifies the 100 percent inspection necessary, since a simple weighing would be equivalent to a density determination. As a second check, compression testing of an appropriate sample size could verify the quality level of the disc material. Appendix A is a recommended procedure for preparation of the cellular structures and their quality control. This could assist in the efficient manufacture of energy dissipation elements.

Cellular Material Density

The wax-aggregate compaction method for control of the apparent density of cellular structures is an effective and practical one. The observed trend toward lower specific energy values, however, was contrary to the primary objectives which were set for these materials. For this reason, only a limited effort was expended toward development of the compacted aggregate structures. It is possible that requirements for lower density structures may develop in the future and, therefore, some discussion of the nature of these structures would be in order.

The method employed for compaction of the structure results in flattening of the otherwise equiaxed cells. The structures which were evaluated, however, represent only a modest departure from those produced by loose packing, and the change in cell geometry is minor. Experience obtained during this study indicated that the lower apparent density material lacked promise for attainment of high specific energy dissipation. Several samples which were prepared and tested at density levels in the 0.3 to 0.4 g/cc range showed relatively low specific energy values at 70 percent deformation. This suggests that any requirement for lower density cellular aluminum structures could only be satisfied at some substantial compromise in specific energy dissipation capacity.

Design of Energy Dissipation Devices

Energy dissipation devices which employ compressible materials, such as cellular aluminum, can be designed in two general ways. In one, an unconfined column is crushed. This leads to consideration of buckling and shear as failure mechanisms, limiting the choice of column geometry (L/D ratio). It also focuses attention on cellular structures and material properties which minimize buckling and shear. This report is almost wholly concerned with the interaction of this design concept with material parameters.

However, there is an equally valid alternate design concept. In this second type of device, the cellular material could also be crushed, but in a state of confinement. By this means, shear and buckling can be eliminated as matters of interest, and material parameters can be optimized purely on crushing characteristics.

The design possibilities associated with this second concept are broad, but the scope of the investigation did not permit consideration of these matters. One design possibility, however, is suggested as an illustration of how material behavior can be related to the design of a device intended to make use of its special characteristics. This design concept is related to the compressive deformation of cellular aluminum in a state of confinement. The employment of the device results in the attainment of the "ideal" load deformation behavior which was unattainable with crushing of unconfined columns. This design possibility is demonstrated and discussed in Appendix B of this report.

CONCLUSIONS

On the basis of the earlier work and this continuation of the study of compressive behavior of cellular aluminum alloys, it may be concluded that

1. High specific energy dissipation characteristics are associated with (a) high compressive yield strength; and (b) high apparent density.

2. The principal mode of catastrophic failure associated with compression of ductile cellular aluminum cylinders is columnar instability and appears which the length to diameter ratio (L/D) is greater than 2.0.

3. The principal mode of catastrophic failure associated with compression of brittle cellular aluminum cylinders is the development of shear planes at relatively low deformation.

4. Catastrophic failure of brittle cellular aluminum material can be inhibited by (a) low L/D ratio (0.2 to 0.5) and (b) stacked-disc construction.

5. Stacked-disc construction of brittle cellular aluminum material permits L/D ratios up to 2.0.

6. Catastrophic failure (columnar instability or shear) of cellular aluminum can be prevented by confinement of the material during compression.

7. Stacked-disc construction is ineffective in inhibiting shear failure under conditions of nonaxial loading.

APPENDIX A

RECOMMENDED PROCEDURES FOR PREPARATION OF ALUMINUM CELLULAR STRUCTURES FOR ENERGY DISSIPATION APPLICATIONS

I. Materials

1. Molds (gypsum-bonded investment material).

2. Flasks (stainless steel tubing).

3. Patterns

   a. Wax (lost wax method)

   b. Metal (plaster mold method).

4. Aggregate (salt crystals, 99.95% NaCl).

5. Alloys

   a. 7075-T6 (high strength)

   b. Al-7% Mg (high ductility).

II. Molding

1. Expendable pattern method (lost wax).

2. Premanent pattern method (plaster mold).

III. Mold Preparation and Filling

1. Expendable pattern

   a. Autoclaving for wax removal at 20 psi steam pressure

   b. Dry at 400° F (4 to 16 hours)

   c. Cool to room temperature and fill with aggregate (use vibration to insure maximum packing of aggregate).

2. Permanent pattern

Draw pattern and prepare and fill mold; then proceed as in III.1.b and III.1.c.

IV. Sintering of Aggregate

Heat mold to 1250° F (12 to 16 hours).

V. Casting (Infiltration) and Solidification

1. Cast at 1400° F melting temperature, using 20 to 60 psi pressure, depending on mesh size of aggregate.

2. Solidify under pressure with water cooling, as shown in Figure A-1.

Neg: 36.231.S1171/ORD.64

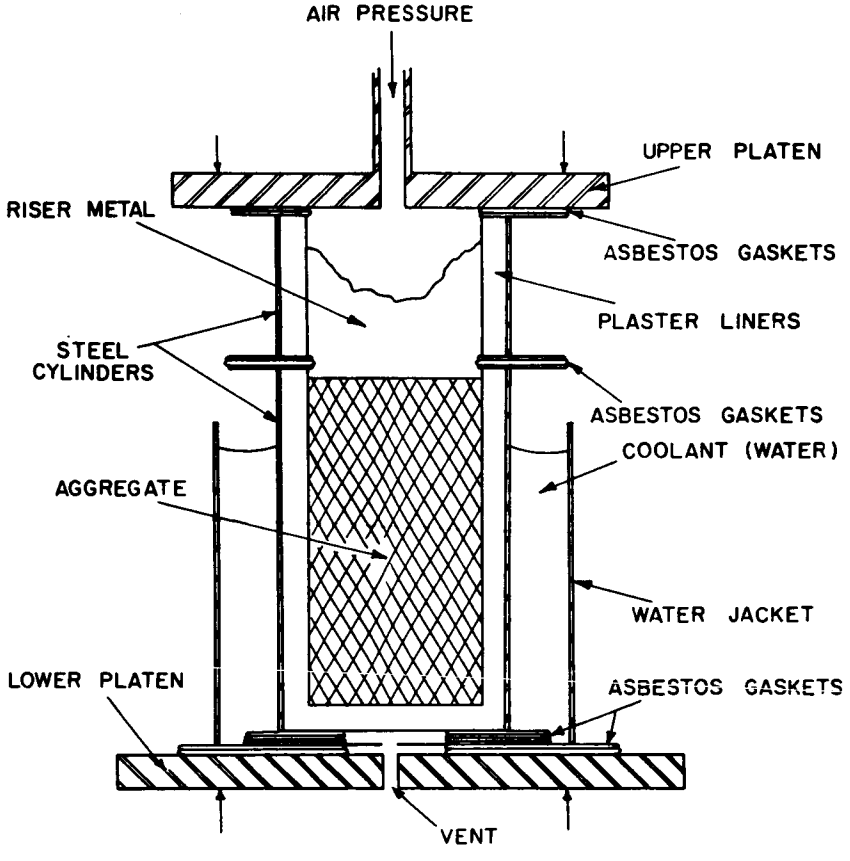

Figure A-1. Schematic illustration of Method for Infiltration of Soluble Aggregate and Solidification of Cellular Metal Castings

VI. Machining.

Use slow speed, sharp tools, and moderately heavy cuts (unleached material).

VII. Heat Treatment

1. Solution-treat component units of cellular metal prior to leaching, in accordance with time and temperature recommended for the alloys.

2. Quench and age to desired temper.

VIII. Leaching

1. Set up leaching operation, as shown in Figure A-2.

Neg. 36.231.S1665/ORD.65

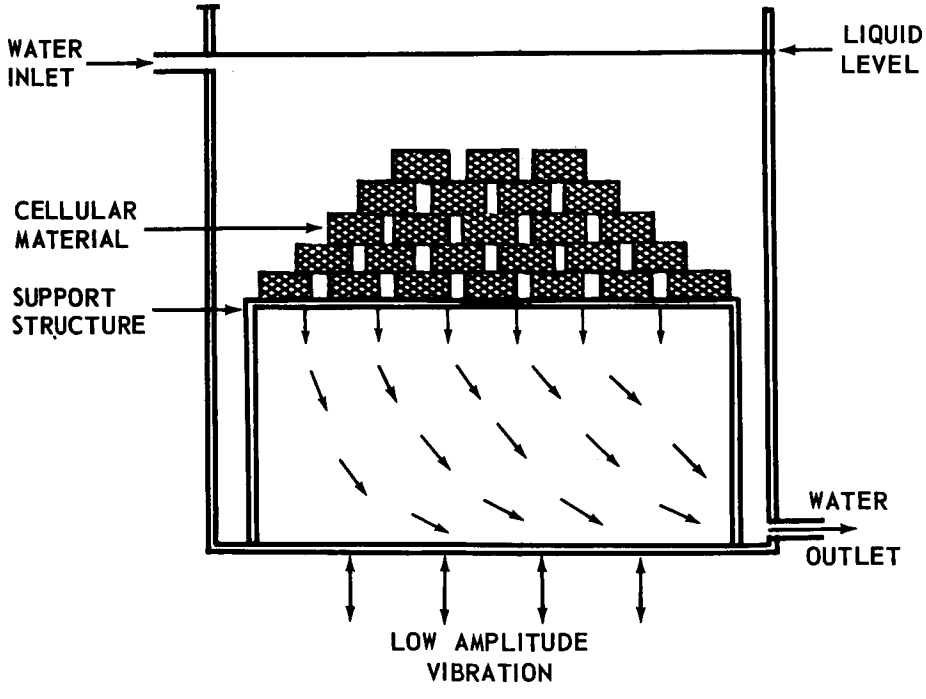

Flow rate: 1/2 change/hour.

Figure A-2. Schematic illustration of Leaching Tank Set-up showing Flow of Salt-laden Liquor

2. Use nonmetallic tank.

3. Support material so that it does not rest on bottom of tank.

4. Use low amplitude vibration to dislodge gas bubbles accumulating in the structure.

5. Replenish liquid at rate of one-half liquid volume change per hour.

6. Check specific gravity of effluent liquor to determine completion of leaching process.

7. Check specific gravity of liquid drained from cellular structure to determine if complete removal of salt has been accomplished.

IX. Drying

Remove liquid (contained in the structure) with centrifuge, and complete drying at ambient temperatures. Incompletely leached material can be detected by salt incrustation on the surface of the material.

X. Quality Control

The mechanical properties of cellular material can be correlated with the apparent density of the material. As a result of this correlation, weight limits can be established for identical components, and the individual component weights can be a basis for selection or rejection. Data contained in the body of this report demonstrate the validity of employing apparent density of the material as a quality criterion.

APPENDIX B

PROPOSED DESIGN FOR LINEAR LOAD ENERGY DISSIPATION DEVICE

Introduction

The requirement for energy dissipation at constant load has been difficult to realize by compression of an unconfined column of the cellular aluminum. In attempting to devise a method whereby energy dissipation could be effected without the load build-up resulting from continued compaction of the compressible material, some consideration was given to the principle of the frangible tube device developed by NASA at Langley Field.*

By substituting a supported cellular metal liner instead of the frangible tube and effecting controlled deformation of the liner by forcing a tapered mandrel through it, the linear load characteristics of the earlier device could be retained. An advantage foreseen for the lined tube is that the structural integrity of the device is maintained and, in fact, even the structural contribution of the liner itself is enhanced during the process of energy dissipation.

Design of Device

Figure B-1 is a schematic illustration of the constant load energy dissipation device. A hollow cellular cylinder is fitted to a supporting tube. Energy dissipation is obtained by forcing the tapered mandrel through the hollow cellular cylinder. The reduction of cross-sectional areas is controlled by the dimensions of the component parts of the system. The actual load necessary to drive the mandrel through the cylinder is affected by the reduction of cylinder area and the compressive properties of the cylinder material. Once the major diameter of the mandrel has entered the cellular cylinder, further increase in load is no longer possible and the energy required to drive the mandrel the remainder of the way through the cylinder is a linear function of the mandrel travel.

Testing of Device

Tests were conducted on 2-inch diameter cylinders having central holes of varying diameters, but no attempt was made to develop design data. A number of cellular cylinders were available from some of the earlier work, and these were tested at two levels of cross-sectional area reduction.

*J. R. McGehee, "A Preliminary Experimental Investigation of an Energy Absorption Process Employing Frangible Metal Tubing," Langley Research Center Technical Note D-1477, Oct 1962.

Neg: 36.231.S1666/ORD.65

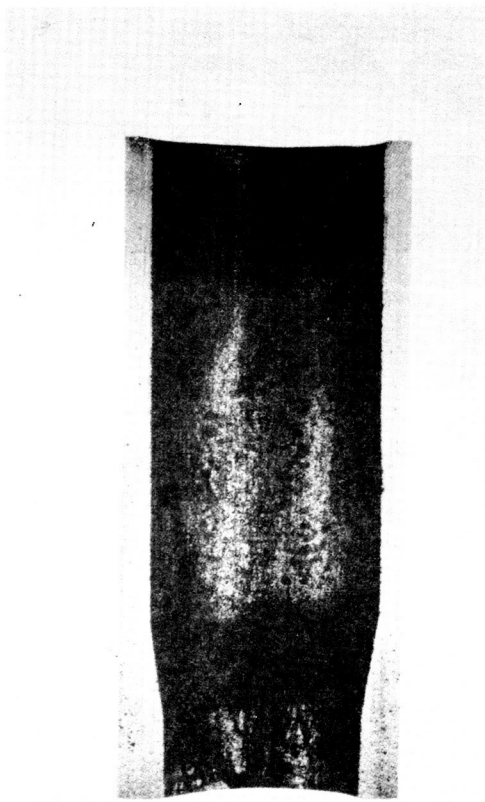

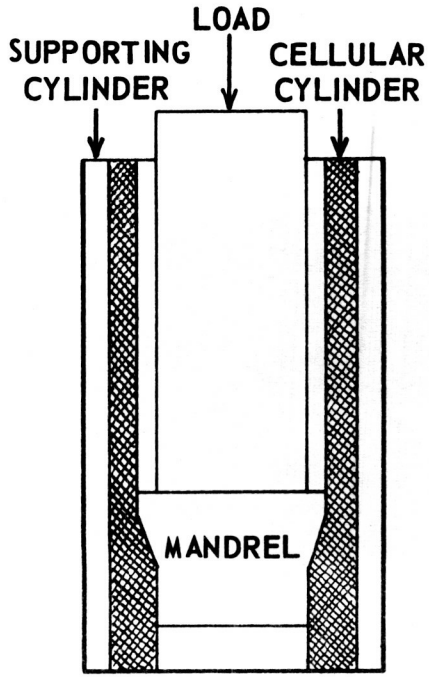

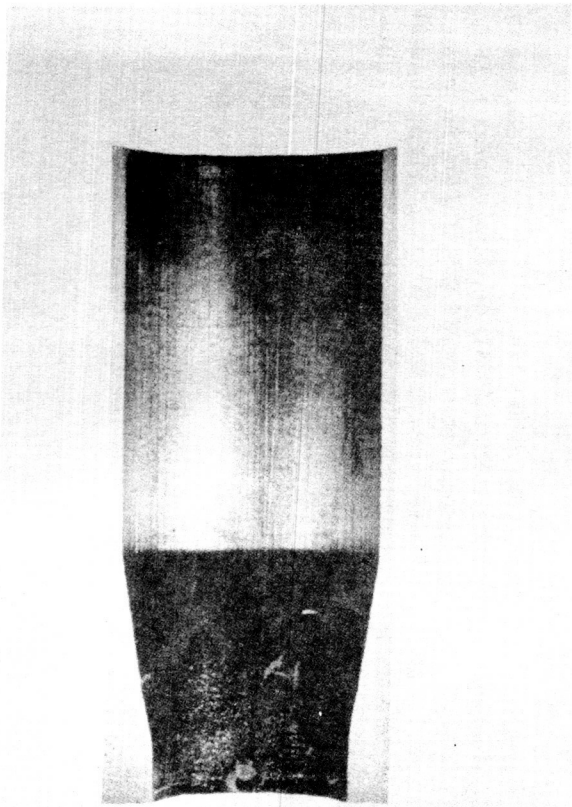

36	Reduction in Area (%)	57
10,000	Specific Energy Dissipation (ft-lb/lb)	31,000
7,500	Load (lb)	27,500

Alloy: Al-7% Mg Cell size: 0.010 in. Cylinder dim: OD - 2.13 in.
Apparent density: 1.0 g/cc ID - 1.50 in.

Figure B-1. Energy Dissipation by Deformation of Cellular Aluminum Cylinder

Figure B-1 shows sections of these deformed cellular cylinders and gives the pertinent data relating to the tests. Since the mandrel is not driven completely through the cylinder, energy dissipation is calculated on the basis of weight of cellular material per unit length and the load needed to drive the mandrel through the cylinder. The weights of the supporting tube and the tapered mandrel are not included.

Figure B-2 is a typical load-deformation record obtained with this device. It is necessary that a lubricant be applied to the mandrel and to the inside surface of the cylinder. Fine graphite in a kerosene vehicle was applied for this purpose.

Neg: 36.231.S1532/ORD.65

Neg: 36.231.S1532/ORD.65

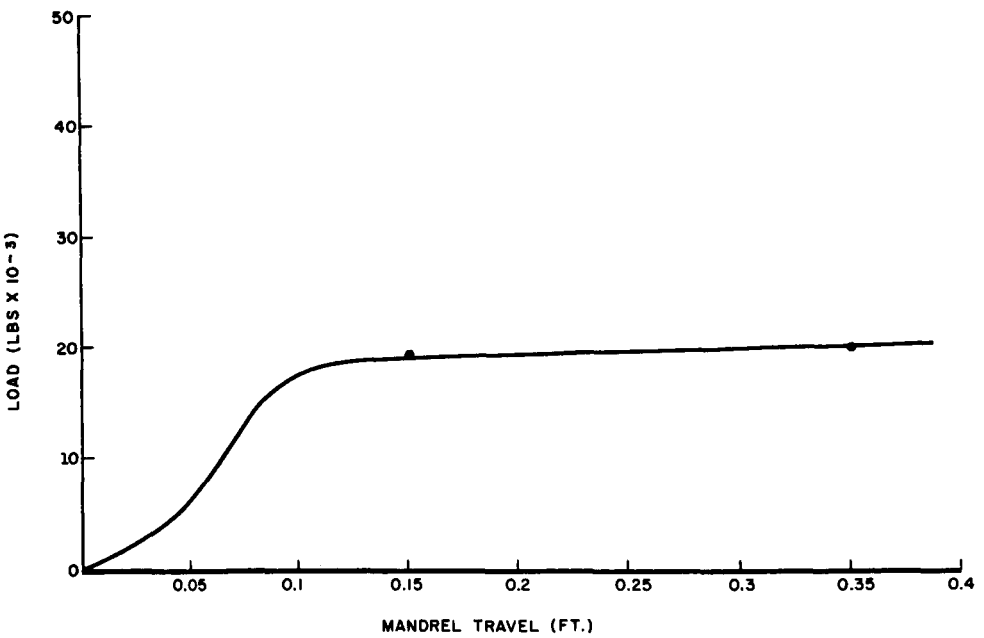

Cellular structure: 12 Mesh, 7075-T6 Tube length: 4.5 inches
Deformation: 29% (reduction in area) Tube weight: 209 g

Figure B-2. Load-deformation Record of Linear Energy Dissipation Device

DISTRIBUTION

U.S.Army

1 - Hq, U.S.Army Materiel Command
Attn: AMCRD-DE-W
Washington, D. C. 20315

1 - Attn AMCRD-DE-MO

1 - Attn: AMCPM

1 - Commanding General
U.S.Army Munitions Command
Attn: Technical Information Div
Dover, N. J. 07801

1 - Attn: AMSMU-RE-E

1 - Attn: AMSMU-RE-A

1 - Attn: AMSMU-RE-N

1 - Attn: AMSMU-RE-P

1 - Attn: AMSMU-LA, USAF Liaison Off

1 - Attn: AMSMU-LC, CDC Liaison Office

1 - Attn: AMSMU-LM, USMC Liaison Off

1 - Hq, U.S.Army Mobility Command
Attn: Technical Information Div
Warren, Mich. 48090

1 - Attn: AMSMO-RR

1 - Attn: AMSMO-RD

1 - Attn: AMSMO-RL

1 - Attn: AMSMO-PR

1 - Attn: Liaison Office, CDC

1 - U.S.Army Natick Laboratory
Attn: AMXRD-ADED
Natick, Mass. 01762

1 - Hq, U.S.Army Test & Evaluation Command
Attn: Dir, Aviation Mat'l Testing
Aberdeen Proving Ground, Md. 21005

1 - Attn: Dir, Gen'l Equipment Testing

1 - Attn: Liaison Office, CDC

2 - Commanding Officer
Attn: Technical Library, Bldg 313
Aberdeen Proving Ground, Md. 21005

1 - Hq, U.S.Army Weapons Command
Attn: Chief Scientist, AMSWE-SAS
Rock Island Arsenal
Rock Island, Ill. 61202

1 - Attn: Technical Information Div

1 - Hq, U.S.Army Missile Command
Attn: Dir, Res & Dev,Directorate
Redstone Arsenal
Huntsville, Ala. 35809

1 - Hq, U.S.Army Electronics Command
Attn: Dir, Res & Dev, AMSEL-RD
Fort Monmouth, N.J. 07703

1 - Hq, U.S.Army Supply and Maintenance Command
Attn: Dir of Maintenance, AMSSM-M
Washington 25, D. C.

1 - Attn: Dir of Supply, AMSSM-S

1 - Hq, U.S.Army Aviation & Surface Materiel Command
Attn: Technical Director
P.O. Box 209, Main Office
St. Louis, Mo. 63166

1 - Attn: Director, Engineering

1 - Attn: Liaison Office, CDC

1 - Hq, U.S.Army Combat Development Command
Attn: Scientific Advisor, CDCSA
Fort Belvoir, Va. 22060

1 - Attn: Directorate of Evaluations CDCRE

1 - Attn: Directorate of Plans, CDCPL

1 - Attn: Directorate of Doctrine, CDCCD

1 - Attn: Directorate of Materiel CDCMR

1 - Attn: Directorate of Organization CDCDO

1 - Commanding Officer
Rock Island Arsenal
Attn: Technical Director
Rock Island, Ill. 61202

1 - Attn: Ch, Design Engineering Br SWERI-RDD

1 - Commanding Officer
Picatinny Arsenal
Attn: Technical Director
Dover, N. J. 07801

1 - Commanding Officer
U.S. Army Research & Development Laboratory
Edgewood Arsenal, Md. 21010

1 - Commanding Officer
U.S.Army Research Office-Durham
Attn: CRD-AA-E
Box CM, Duke Station
Durham, N. C. 27706

1 - Attn: CRD-AA-X

1 - U.S.Army Field Office
Space Systems Div (AFSC)
AF Unit Post Office
Los Angeles, Calif. 90045

1 - Commanding Officer
Harry Diamond Laboratories
Attn: Technical Director
Washington, D. C. 20438

1 - Attn: AMXDO TIB

1 - Commanding General
U.S.Army Aviation Center
Attn: Director, USAATBG
Fort Rucker, Ala.

1 - Attn: Director, USAATHRE

1 - Attn: Director, USABAAR

1 - Commanding Officer
U.S.Army Transportation Research Command
Attn: Technical Director
Fort Eustis, Va. 23604

National Aeronautics & Space Adm

1 - Dir, NASA Langley Research Center
Attn: Mrs. E. R. Gilman, Librarian
Langley Station
Hampton, Va. 23365

5 - Attn: Structures Res Div, L.J.Fisher

1 - Director, NASA Goddard Space Flight Center
Greenbelt, Md. 20771

1 - Director, NASA Jet Propulsion Laboratory
Pasadena, Calif.

1 - Director, NASA Lewis Research Center
Cleveland, Ohio 44111

1 - Dir, NASA Geo. C. Marshall
Space Flight Center
Attn: Saturn System Office
Huntsville, Ala. 35809

1 - Attn: Propulsion & Energy Div

1 - Attn: Future Projects Office

1 - Attn: Research Projects Office

1 - Dir, NASA Manned Spacecraft Center
Attn: Gemini Spacecraft Proj Off
Houston, Texas 77058

2 - Attn: Mr. Chas. M. Grant, Jr.
Ch, Technical Inf Div
Code ACI

2 - Attn: Project Mercury Office

2 - Attn: Apollo Spacecraft Proj Off

1 - Attn: Office of Asst Director,
Research & Development

1 - Attn: Spacecraft Research Div

1 - Attn: Crew System Div

U.S.Navy

1 - Ch, Bureau of Naval Weapons
Department of the Navy
Attn: RMMO
Washington, D. C. 20360

1 - Attn: RMMP

1 - Commanding Officer
U.S.Naval Weapons Laboratory
Attn: J. Glancy, Code TC
Dahlgren, Va. 22448

1 - Commanding Officer
U.S.Naval Ordnance Test Station
Attn: D. Strietzel, Code 4574
China Lake, Calif.

1 - Commanding Officer
U.S.Naval Ordnance Plant
Attn: Code PD-270
Macon, Ga.

1 - Dir, Air Crew Equipment Laboratory
Naval Air Engineering Center
Attn: C. T. Koochembere, Gr Mgr
Philadelphia, Pa. 19112

1 - Commander
Naval Air Development Center
Attn: Technical Library
Johnsville, Pa. 18974

U.S. Air Force

3 - Cmdr, AF Flight Dynamics Laboratory
Attn: Mr. R. Dobbek (FDFR)
Wright-Patterson AFB, Ohio 45433

2 - Systems Engineering Group
Attn: SEMCS, Mr. C. Snyder
Wright-Patterson AFB, Ohio 45433

1 - Attn: SEPIE

1 - Attn: SEPIR

1 - Attn: SEMHD, Mr. Chas. H. Moser

1 - Attn: SEMEP, Mr. C. E. Grindstaff

1 - Attn: SEMES, Mr. C. K. Hodell

1 - Attn: Directorate of Technical
Publications & Specifications
SEPRR

1 - AF Materials Laboratories
Attn: MRBAV, Maj. N. P. Clarke
Wright-Patterson AFB, Ohio 45433

1 - Life Support Systems, SPO (412-A)
Attn: ASWL, Mr. A. H. Rosner
Wright-Patterson AFB, Ohio 45433

1 - Aeronautical Systems Div
Attn: ASZJE, Mr. E. Dock
Wright-Patterson AFB, Ohio 45433

1 - Attn: ASZWE, Maj. F. H. Briggs

1 - Attn: ASZFO-A

1 - Attn: Deputy forF-111 (ASLE)

1 - Directorate of Aerospace Safety
Attn: Ch, Life Sciences Group
AFIAS-L
Norton Air Force Base, Calif. 92409

1 - Commander
Ogden Air Materiel Area
Attn: OONEAA
Hill Air Force Base, Utah

1 - Commander
2705th Airmunitions Wing (AMC)
Attn: OOYTC
Hill Air Force Base, Utah

1 - Commander
Edwards Air Force Base
Attn: AFRPL (RPMM)
Edwards, Calif. 93523

1 - USAF Special Weapons Center
Attn: SWOI
Kirtland Air Force Base, N.M.

1 - Commander
Air University Library, USAF
Attn: 2-T-AU2-60-118
Maxwell Air Force Base, Ala.

1 - Hq, USAF (AFXSAI)
The Pentagon
Washington, D. C. 20301

OTHER

20 - Defense Documentation Center
Cameron Station
Alexandria, Va. 22314

1 - Chemical Propulsion Information Agency
Johns Hopkins University
Silver Spring, Md. 20910

2 - Scientific & Technical Information Facility
Attn: NASA Representative (S-AK/DL)
P.O. Box 5700
Bethesda, Md. 22014

Publications Branch
FRANKFORD ARSENAL
Date Printed: 1/21/66

UNCLASSIFIED

Security Classification

DOCUMENT CONTROL DATA - R&D

(Security classification of title, body of abstract and indexing annotation must be entered when the overall report is classified)

1. ORIGINATING ACTIVITY *(Corporate author)* FRANKFORD ARSENAL, Philadelphia, Pa. 19137 Attn: SMUFA L3100	2a. REPORT SECURITY CLASSIFICATION Unclassified 2b. GROUP NA

3. REPORT TITLE

ENERGY ABSORPTION PROPERTIES OF CELLULAR ALUMINUM

4. DESCRIPTIVE NOTES *(Type of report and inclusive dates)*

Technical Research Report

5. AUTHOR*(S) (Last name, first name, initial)*

LIPSON, Samuel

6. REPORT DATE November 1965	7a. TOTAL NO. OF PAGES 36	7b. NO. OF REFS Two
8a. CONTRACT OR GRANT NO. NASA Purchase Request L-18,381 b. PROJECT NO. c. d.	9a. ORIGINATOR'S REPORT NUMBER*(S)* R-1784 9b. OTHER REPORT NO*(S) (Any other numbers that may be assigned this report)*	

10. AVAILABILITY/LIMITATION NOTICES

Distribution of this report is unlimited.

11. SUPPLEMENTARY NOTES	12. SPONSORING MILITARY ACTIVITY NASA Langley Research Center

13. ABSTRACT

The scope of this study covers the optimization of materials and structures of cellular aluminum with respect to applications requiring controlled dissipation of kinetic energy. A design of a linear energy dissipation system is suggested, and its effective operation is demonstrated. Conclusions are presented relative to the effect of material properties on energy dissipation characteristics.

DD FORM 1 JAN 64 1473

UNCLASSIFIED

Security Classification

14. KEY WORDS	LINK A ROLE	LINK A WT	LINK B ROLE	LINK B WT	LINK C ROLE	LINK C WT
Energy Dissipation						
Cellular Aluminum						
Compressive Properties						
Radial Compression						
Linear Compression						
Heat Treatment						
Lightweight Structures						
Porous Metals						
Porosity						
Density						
Cell Size						
Leaching						

INSTRUCTIONS

1. ORIGINATING ACTIVITY: Enter the name and address of the contractor, subcontractor, grantee, Department of Defense activity or other organization *(corporate author)* issuing the report.

2a. REPORT SECURITY CLASSIFICATION: Enter the overall security classification of the report. Indicate whether "Restricted Data" is included. Marking is to be in accordance with appropriate security regulations.

2b. GROUP: Automatic downgrading is specified in DoD Directive 5200.10 and Armed Forces Industrial Manual. Enter the group number. Also, when applicable, show that optional markings have been used for Group 3 and Group 4 as authorized.

3. REPORT TITLE: Enter the complete report title in all capital letters. Titles in all cases should be unclassified. If a meaningful title cannot be selected without classification, show title classification in all capitals in parenthesis immediately following the title.

4. DESCRIPTIVE NOTES: If appropriate, enter the type of report, e.g., interim, progress, summary, annual, or final. Give the inclusive dates when a specific reporting period is covered.

5. AUTHOR(S): Enter the name(s) of author(s) as shown on or in the report. Enter last name, first name, middle initial. If military, show rank and branch of service. The name of the principal author is an absolute minimum requirement.

6. REPORT DATE: Enter the date of the report as day, month, year; or month, year. If more than one date appears on the report, use date of publication.

7a. TOTAL NUMBER OF PAGES: The total page count should follow normal pagination procedures, i.e., enter the number of pages containing information.

7b. NUMBER OF REFERENCES: Enter the total number of references cited in the report.

8a. CONTRACT OR GRANT NUMBER: If appropriate, enter the applicable number of the contract or grant under which the report was written.

8b, 8c, & 8d. PROJECT NUMBER: Enter the appropriate military department identification, such as project number, subproject number, system numbers, task number, etc.

9a. ORIGINATOR'S REPORT NUMBER(S): Enter the official report number by which the document will be identified and controlled by the originating activity. This number must be unique to this report.

9b. OTHER REPORT NUMBER(S): If the report has been assigned any other report numbers *(either by the originator or by the sponsor)*, also enter this number(s).

10. AVAILABILITY/LIMITATION NOTICES: Enter any limitations on further dissemination of the report, other than those imposed by security classification, using standard statements such as:

(1) "Qualified requesters may obtain copies of this report from DDC."

(2) "Foreign announcement and dissemination of this report by DDC is not authorized."

(3) "U. S. Government agencies may obtain copies of this report directly from DDC. Other qualified DDC users shall request through _____."

(4) "U. S. military agencies may obtain copies of this report directly from DDC. Other qualified users shall request through _____."

(5) "All distribution of this report is controlled. Qualified DDC users shall request through _____."

If the report has been furnished to the Office of Technical Services, Department of Commerce, for sale to the public, indicate this fact and enter the price, if known.

11. SUPPLEMENTARY NOTES: Use for additional explanatory notes.

12. SPONSORING MILITARY ACTIVITY: Enter the name of the departmental project office or laboratory sponsoring *(paying for)* the research and development. Include address.

13. ABSTRACT: Enter an abstract giving a brief and factual summary of the document indicative of the report, even though it may also appear elsewhere in the body of the technical report. If additional space is required, a continuation sheet shall be attached.

It is highly desirable that the abstract of classified reports be unclassified. Each paragraph of the abstract shall end with an indication of the military security classification of the information in the paragraph, represented as *(TS)*, *(S)*, *(C)*, or *(U)*.

There is no limitation on the length of the abstract. However, the suggested length is from 150 to 225 words.

14. KEY WORDS: Key words are technically meaningful terms or short phrases that characterize a report and may be used as index entries for cataloging the report. Key words must be selected so that no security classification is required. Idenfiers, such as equipment model designation, trade name, military project code name, geographic location, may be used as key words but will be followed by an indication of technical context. The assignment of links, rules, and weights is optional.